Construction and Building Materials 453 (2024) 138890

Contents lists available at ScienceDirect

Construction and Building Materials

journal homepage: www.elsevier.com/locate/conbuildmat

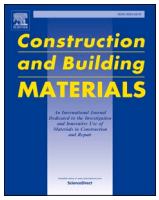

Natural fibers as promising core materials of vacuum insulation panels

Rui Zhang [a], Zhenglai Shen [a], Bokyung Park [a], Tianli Feng [b], Antonio Aldykiewicz Jr. [a], André Desjarlais [a], Diana Hun [a], Som Shrestha [a,*]

[a] Buildings and Transportation Science Division, Oak Ridge National Laboratory, Oak Ridge, TN 37831, USA
[b] Department of Mechanical Engineering, University of Utah, Salt Lake City, UT 84112, USA

ARTICLE INFO

Keywords:
Natural fiber
Vacuum insulation panel
Core material
Thermal conductivity
Building energy efficiency

ABSTRACT

To reduce energy *consumption* in buildings, this paper investigates the feasibility of using natural fibers as cost-effective, environmentally sustainable core materials for vacuum insulation panels (VIPs). First, a comprehensive experimental study was conducted for 10 potential natural fiber candidates. The thermal conductivities of the 10 natural fiber mats at various vacuum pressures were measured; their compression and morphology properties were quantified. In addition, an analytical model was used to explore the major factors that influence the thermal conductivity of natural fibers as a function of internal air pressure. Results show that recycled cotton, kapok, and bamboo fibers are ideal candidates for VIP core materials; at <0.05 Pa, their thermal conductivities varied between 2 and 4 mW/(m·K). Furthermore, for some fibers, thermal conductivity was inversely proportional to fiber density. For the selection of fiber materials for VIP cores, the ideal fiber candidate has a small fiber diameter and a low fiber mat density. Based on thermal measurements, even though the internal air pressure of 5 Pa was enough to attain the minimum thermal conductivity, obtaining internal air pressure below 5 Pa is recommended for prolonged service life, considering small leaks of VIP package barrier films and potential off-gassing from fibers. The simulation results predicting the effective thermal conductivities matched the experimental results well. These findings indicate that natural fiber–based VIPs have the potential to be a sustainable, inexpensive alternative to the current technologies in building insulation materials.

1. Introduction

In response to the challenges posed by climate change, the United States aims to achieve net-zero greenhouse gas emissions by 2050 [1]. Among greenhouse gas emissions contributors, the building sector is responsible for about 30 % of greenhouse gas emissions and 40 % of energy consumption worldwide [2,3]. Increasing the thermal resistance (R-value) of the building envelope is an effective way to decrease heat loss, improve building energy efficiency, and reduce operational emissions. Among the various ways to increase the R-value of the building envelope, vacuum insulation panels (VIPs) offer significant promise. They have three to six times higher thermal resistivity than that of traditional building insulation materials [4] and thus can be 67 %–83 % thinner while achieving the same insulation performance; VIPs therefore offer notable advantages in reducing construction space usage [5]. The implementation of VIPs in office buildings reduces annual energy demand. For example, several projects in London reduced energy consumption by 10.2 %–26.7 % [6]. VIPs used in envelope retrofits for commercial buildings reduced energy consumption by approximately 35 % compared with the consumption of pre-retrofit conditions in Sweden and Spain [7]. However, VIPs are not widely adopted in building insulation because of their high cost [8–10].

A VIP (shown in Fig. 1) comprises an inner core with or without getters and desiccants and a barrier envelope that includes a porous bag and a barrier film; the core material is the VIP's main cost driver [11]. Common VIP core materials include porous foams (e.g., polyurethane and polystyrene), powders (e.g., fumed silica), silica aerogels, expanded perlite, and fiberglass [12]. The most commonly used core material, fumed silica, costs around $3.70/kg–$5.00/kg, which may vary depending on when the material was purchased [13–16]. In addition to silica's high cost, exposure to amorphous silica has been linked to respiratory illnesses such as fibrosis [17].

Natural fibers offer an economical and sustainable alternative to current commonly used VIP core materials because of their low cost, low environmental impact, and good thermal performance [18]. Jute, kenaf, coir, hemp, and bamboo prices ($0.24/kg–$0.70/kg) would provide an 80 %–90 % discount compared with traditional VIP core material prices

* Corresponding author.
E-mail address: shresthass@ornl.gov (S. Shrestha).

https://doi.org/10.1016/j.conbuildmat.2024.138890
Received 5 April 2024; Received in revised form 26 August 2024; Accepted 20 October 2024

Nomenclature

Abbreviations

HFM	Heat flow meter
MSE	Mean squared error
SEM	Scanning electron microscopy
VIP	Vacuum insulation panel

Symbols

λ_{eff}	Effective thermal conductivity (mW/[m·K])
λ_G	Thermal conductivity due to gas conduction (mW/[m·K])
λ_F	Thermal conductivity due to solid conduction (mW/[m·K])
λ_R	Thermal conductivity due to radiation in the fibers (mW/[m·K])
λ_g	Thermal conductivity of the gas (mW/[m·K])
λ_s	Thermal conductivity of the solid (mW/[m·K])
$\lambda_{g,0}$	Thermal conductivity of air at diffusive limit at 297 K (26 mW/[m·K])
p	Internal air pressure (Pa)
T	Internal air temperature (K)
E	Constant for a specific gas ($E = 2.332 \times 10^{-5}$ for air)
D	Fiber diameter (m)
L_0	Mean fiber distance (m)
f	Fraction of the fiber considered parallel to the heat flow
ϕ_P	Porosity structure parameters in parallel
ϕ_S	Porosity structure parameters in series
ϕ	Porosity of the fiber mat
ρ	Bulk density of the fiber mat (kg/m^3)
ρ_s	Density of the solid phase (kg/m^3)
σ_S	Stefan–Boltzmann constant ($\sigma_S = 5.67 \times 10^{-8}$ W/[m^2·K^4])
β	Opacity factor
T_m	Average measured temperature of the fiber mat in the heat flow meter (T_m = 297.039 K)

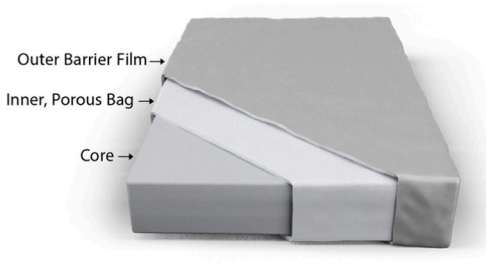

Fig. 1. Schematic diagram of a VIP.

[19]. As renewable plant resources, these natural fibers sequester CO_2 while growing. Additionally, they are biodegradable at the end of their life cycles. Although numerous studies have measured the thermal conductivities of natural fibers—such as blue jeans, wool felt, coconut jute, sheep wool, and jute mat—at ambient air pressure [18–25], few have investigated the thermal conductivities of natural fibers at reduced air pressure [14,19,26,27]. Likewise, very few studies have evaluated whether an internal supportive structure can improve the thermal performance of VIPs using natural fibers as the core material [28–30]. Overall, a comprehensive evaluation of the potential of natural-fiber VIP core materials is lacking.

The purpose of this paper is to identify and compare potential candidates of natural fiber–based VIP core materials that can deliver similar or better thermal performance compared with that of conventional VIP core materials. A comprehensive experimental study together with analytical modeling was used to evaluate and predict the performance of natural fibers as VIP core material.

Ten natural fiber materials were selected, and their thermal conductivities over vacuum pressures of 0.01–10 Pa were measured. Compressive tests were performed to study the density change with external compressive pressure and to determine whether an internal support structure is required to maintain the porous structure of the VIP core. Furthermore, an analytical model was calibrated by experimental thermal conductivity data and used to find the key design parameters of natural fiber–based VIPs. The analytical model considers contributions from the gas, the solid, and the radiation to effective thermal conductivity. This study fills the knowledge gap concerning the feasibility of employing various natural fibers as VIP core materials and thus contributes to the development of efficient, sustainable, low-cost insulation solutions.

2. Methodology

2.1. Materials and sample preparation

Ten natural fibers were selected, including blue jeans from denim waste (a type of cotton waste), recycled cotton, tan wool felt, coconut shell jute, kapok, three types of sheep wool batt (high density [#1], low density [#2], and medium density [#3]), bamboo fiber, and jute mat, as shown in Fig. 2. The three sheep wool batts are animal fibers, and the other materials are plant-based fibers. These natural fibers were selected because of their availability in the market and their potential to be used as the core materials of VIPs. Moreover, previous thermal tests of these fibers at ambient pressure have indicated their potential viability as insulation materials [18–25,31]. This suggests that these natural fibers could also provide great thermal performance at reduced air pressure as potential candidates for VIP core materials.

As shown in Fig. 3, the natural fibers were first cut into two separate sets of mats: one set was 203.2 × 203.2 mm (8 × 8 in.) square mats for thermal conductivity measurements and another set was 101.6 × 101.6 mm (4 × 4 in.) square mats for compression tests. These sets were to fit into the heat flow meter (HFM) and the compressive instrument. The 203.2 × 203.2 mm (8 × 8 in.) square mats were used for evaluating effects of air pressure and density. To shape the loose-fill natural fibers (kapok, sheep wool batt #2, and bamboo fiber) with their original densities to fit the size of the heat flow meter, these materials were stacked layer by layer into empty 203.2 × 203.2 mm (8 × 8 in.) and 101.6 × 101.6 mm (4 × 4 in.) square boxes. Each material's unique nature resulted in surface variability among the different materials. Then all the samples were dried in an oven at 80°C for at least 12 h to minimize the influence of moisture. Following that, the thicknesses and weights of the specimens were measured to determine their initial densities under a standard laboratory indoor environment. The thickness, weight, and density of each sample are summarized in Table 1. Under different applied external pressures, the thickness measured by HFM was used to calculate each material's density based on its original horizontal cross-section area and mass.

2.2. Thermal performance, mechanical properties, and material characterization

This study experimentally evaluated the thermal conductivities and compressive strengths of and characterized the morphologies of natural fibers as candidate core materials of VIPs.

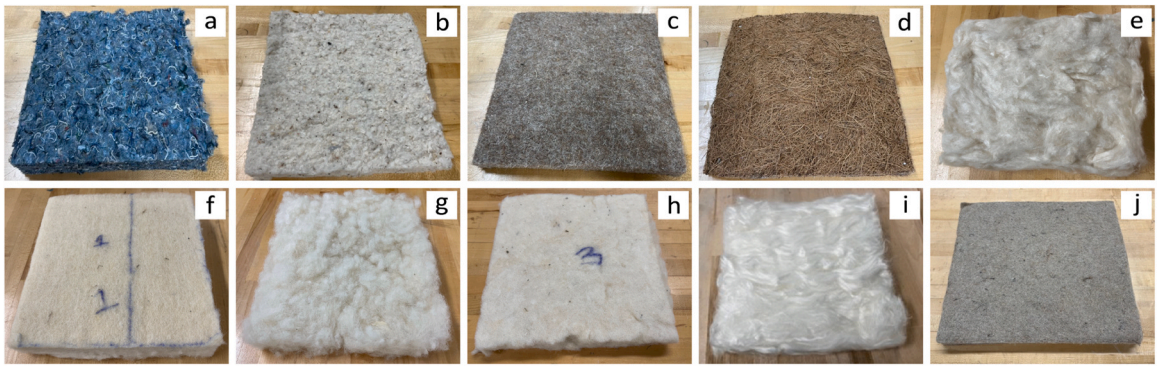

Fig. 2. Selected natural fiber mats: (a) blue jeans, (b) recycled cotton, (c) tan wool felt, (d) coconut jute, (e) kapok, (f) sheep wool batt #1, (g) sheep wool batt #2, (h) sheep wool batt #3, (i) bamboo fiber, and (j) jute mat.

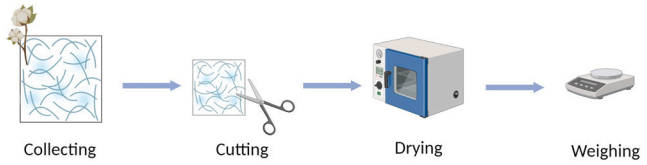

Fig. 3. Fiber mat preparation (image created with BioRender.com.).

2.2.1. Thermal conductivity measurement

Thermal conductivity was measured by an HFM in accordance with ASTM C518, *Standard Test Method for Steady-State Thermal Transmission Properties by Means of the Heat Flow Meter Apparatus* [32]. The HFM was covered by an airtight cover and connected to a roughing pump and a turbo pump to adjust the vacuum pressure levels, as shown in Fig. 4(a). The HFM used in this study was made by TA Instruments. A 25.4 mm (1 in.) thick standard reference material 1450b board (from the National Institute of Standards and Technology) was used to calibrate the HFM before conducting the thermal conductivity measurements. There were two equilibrium criteria for thermal conductivity measurements: (1) the average temperature of each HFM plate in the block is within ± 0.2°C of the setpoint temperature; and (2) the difference in the heat flux transducers' average signals of two successive blocks must be within 40 μV and 3 %. The last five blocks of the data were used to calculate thermal conductivity. For all measured samples, the mean standard deviation was 0.032 mW/(m·K).

The sample (fiber mat) was placed between the HFM's upper and lower plates, which were equipped with independently controlled heating and cooling elements. Heat flux sensors were installed in the plates to measure the heat flow. During the test, the upper and lower plates were set to 12.8°C and 35°C, respectively, resulting in a temperature difference of 22.2°C and a mean temperature of 23.9°C. The thermal conductivity was measured at various pressures from 101,325 Pa (the ambient air pressure) to a minimum pressure of approximately 0.01 Pa. When operating only the roughing pump, the HFM internal air pressure decreased to 10 Pa. Operating both the roughing pump and the turbo pump reduced the pressure to approximately 0.01 Pa.

At each air pressure level, various material densities could be evaluated by controlling the distance between the HFM plates from no compression to the maximum compression applied on the test sample, as shown in Fig. 4(b). When the HFM was set to auto thickness mode, the upper plate compressed the test sample by applying a maximum pressure of 6205 Pa. Under this applied load, the test sample achieved the minimum thickness and the maximum density. When the HFM was set to manual thickness mode, the sample thickness varied from the maximum value (without an external force—0 Pa) to the achievable minimum value (with the upper plate force—6205 Pa). By changing the thickness, we studied the effect of density on the thermal conductivity.

2.2.2. Compression test

Compression tests were conducted to obtain measurements of the density change under different external pressures and to evaluate whether the studied natural fiber–based VIPs need internal support structures to prevent the core from being crushed by atmospheric pressure or external forces. The INSTRON 3340, which has a maximum compression force of 1000 N, was used following ASTM C165, *Standard Test Method for Measuring Compressive Properties of Thermal Insulations*

Table 1
Summary of samples (101.6 mm width and 101.6 mm length) and their densities under different external applied pressures.

Material	Thickness (mm)	Mass (g)	Density, ρ, under an external pressure (kg/m^3)			$\frac{\rho_{6kPa} - \rho_{0\ kPa}}{\rho_{0\ kPa}}$	$\frac{\rho_{101\ kPa} - \rho_{0\ kPa}}{\rho_{0\ kPa}}$
			0 kPa[a]	6 kPa[b]	101 kPa[c]		
Blue jeans	31.8	49.8	38.0	76.0	256.9	100 %	576 %
Recycled cotton	31.8	64.1	52	93	213	78 %	308 %
Tan wool felt	18.9	148.2	190	196	241	3 %	27 %
Coconut jute	11.7	57.1	118	125	N/A[d]	6 %	N/A[d]
Kapok	38.1	27.1	17	46	188	169 %	991 %
Sheep wool batt #1	64.0	89.0	37	115	236	214 %	544 %
Sheep wool batt #2	45.1	23.3	11	67	300	523 %	2702 %
Sheep wool batt #3	56.6	68.8	32	108	258	243 %	718 %
Bamboo fiber	32.9	51.3	37	205	496	461 %	1255 %
Jute mat	31.0	130.2	102	126	196	24 %	92 %

[a] The initial density of the fiber mat without any external pressure at 0 Pa.
[b] The density of the fiber mat, which was compressed by the upper plate of the heat flow meter under an external pressure at 6205 Pa.
[c] The density of the fiber mat under an external pressure at 101,325 Pa, which mimicked the mat's density as a VIP core material in the absence of any internal VIP support structure. The external wall of the VIP package experienced the application of atmospheric pressure, resulting in compression of the mat.
[d] Compression test was not performed on coconut jute because of its poor thermal performance compared with that of the other materials.

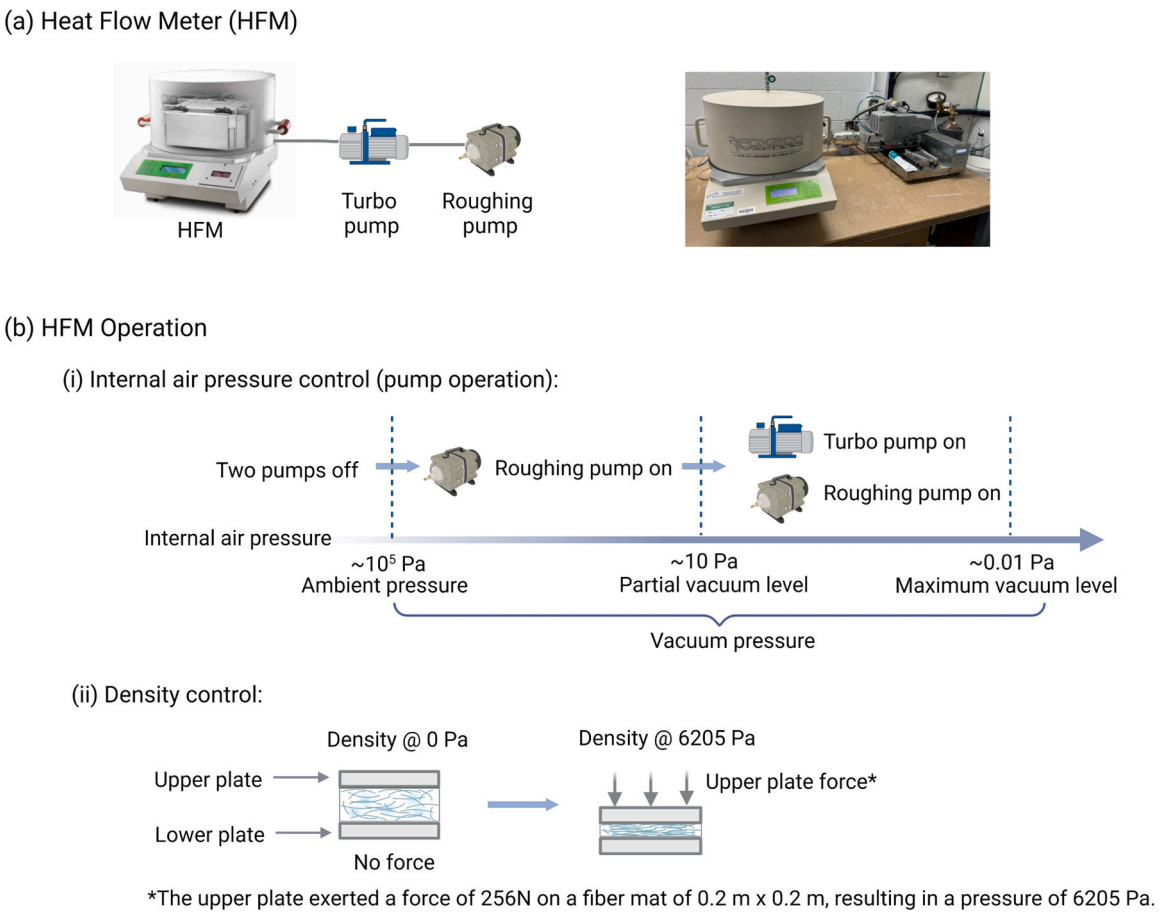

Fig. 4. Instruments and operation for thermal conductivity measurements: (a) HFM and (b) HFM operation (image created with BioRender.com).

[33]. The 101.6 × 101.6 mm^2 test samples were sandwiched between the upper and lower plates. A compressive load was applied at a rate of 103.26 N/min, and the corresponding deformation was recorded. The stress–strain curves were generated by normalizing compressive load to sample area and plotting compressive load as a function of deformation. Modulus of elasticity was calculated by using the initial linear portion of the stress–strain curve. Additionally, the density was obtained based on the thickness of the fiber mat under different compressive loads.

2.2.3. Fiber morphology

Fiber morphology plays a significant role in the performance of the VIP fiber mat, influencing the VIP's thermal conductivity. We examined the morphologies of the fiber mats by using a scanning electron microscopy (SEM) instrument (TESCAN MIRA3). It was equipped with a secondary electron detector and operated at a 2.0 kV accelerating voltage. Before taking SEM imaging, the mats were coated with a thin layer of carbon to increase the signal-to-noise ratio for the purpose of improving image quality. The SEM images were analyzed using ImageJ software; the diameter of each fiber was measured in over 100 locations at a magnification of ×300 using the line selection tool. The average diameter and standard deviation for each fiber were obtained.

2.3. Model description

To gain a deeper understanding of heat transfer in natural fiber–based VIPs, an analytical model was calibrated by the measured thermal conductivities of fiber-based materials. It assessed the applicability of existing heat transfer models for predicting effective thermal conductivity as a function of vacuum pressure levels. Recycled cotton and blue jeans were selected from groupings of ideal (<4 mW/[m·K]) and excellent (4–8 mW/[m·K]) candidates, respectively, for the calibration because of their accessibility (see Section 3.1.1. for information on the groupings).

For fiber-based materials, the effective thermal conductivity of a VIP core can be calculated as the sum of the conductions of gas, solid fiber, and radiation through the fiber matrix when coupling effects can be ignored for optically thick materials and low gas pressures [26,34–38]. Thus, the effective thermal conductivity, λ_{eff}, is [34]

$$\lambda_{eff} = \lambda_G + \lambda_F + \lambda_R, \# \tag{1}$$

where λ_G, λ_F, and λ_R are the thermal conductivities due to gas conduction, solid conduction, and radiation through the fiber matrix, respectively, with

$$\lambda_G = f \bullet \phi_P \bullet \lambda_g + (1-f) \bullet \frac{\lambda_s \bullet \lambda_g}{\phi_S \bullet \lambda_s + (1-\phi_S) \bullet \lambda_g}, \tag{2}$$

$$\lambda_g = \lambda_{g,0} \bullet \frac{p \bullet L_0}{p \bullet L_0 + E \bullet T}, \tag{3}$$

$$L_0 = \frac{\pi}{4} \bullet \frac{D}{1-\phi}. \tag{4}$$

where

- λ_g and λ_s are the thermal conductivities of the gas and the solid, respectively;
- $\lambda_{g,0}$ is the thermal conductivity of ideal gas (0.026 W/[m·K] [38]);
- p is the gas pressure;
- T is the temperature;
- E is a constant for a certain gas (for air, E is 2.332 × 10^{-5} [34]);

- D is the fiber diameter averaged based on the SEM images;
- L_0 is the mean fiber distance calculated based on the fiber diameter and porosity;
- f is the fraction of the material considered parallel to the heat flow, and $(1-f)$ is the fraction in series with the heat flow; and
- ϕ_P and ϕ_S are the porosity structure parameters in parallel and in series, respectively.

The variables ϕ_P, ϕ_S, and f depend on the material porosity, ϕ, according to

$$\phi = (1-f) \bullet \phi_S + f \bullet \phi_P. \tag{5}$$

The porosity, ϕ, is given by

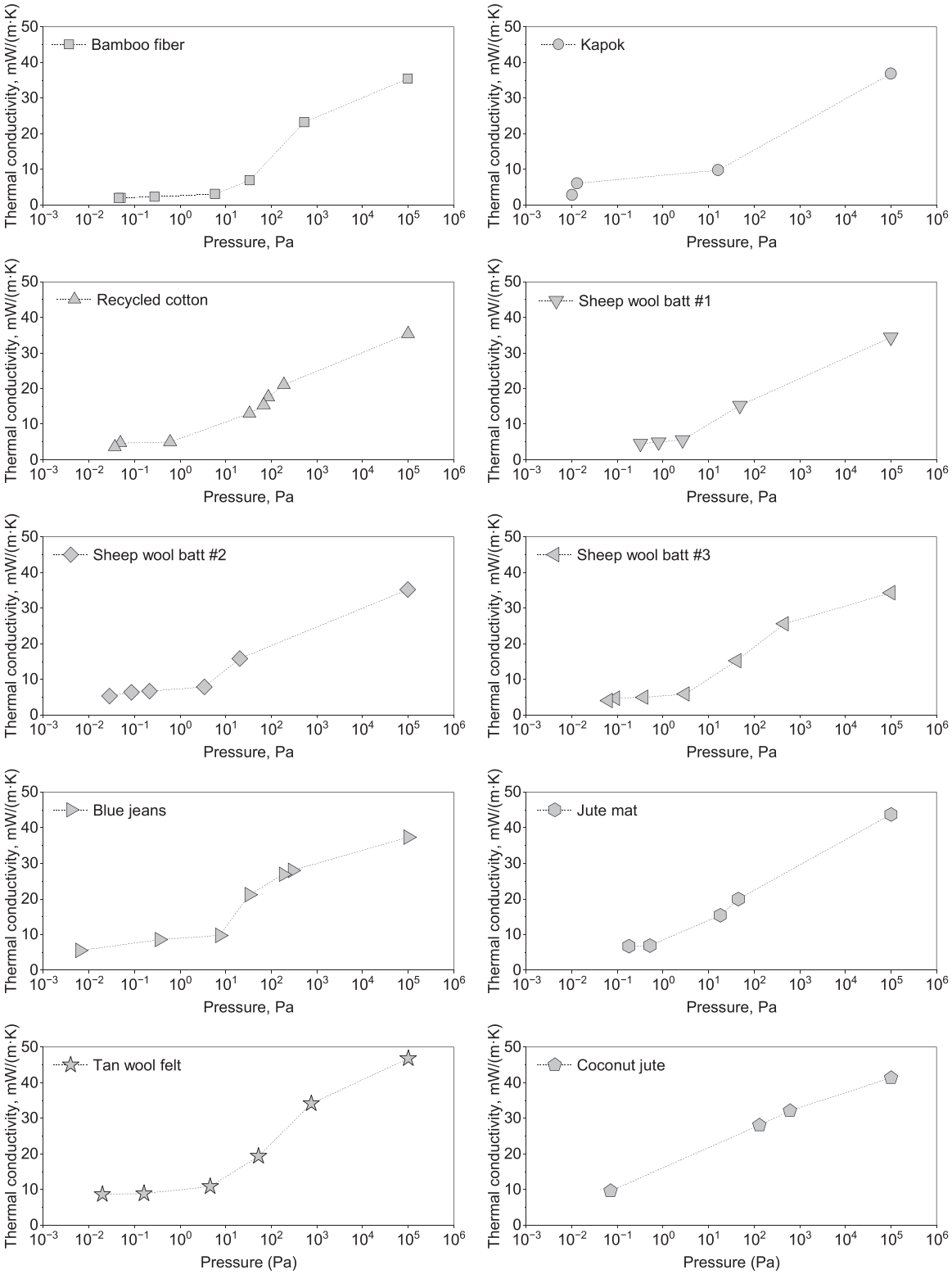

Fig. 5. Measured thermal conductivities of natural fiber mats at various air pressures.

$$\phi = 1 - \frac{\rho}{\rho_s}. \quad (6)$$

where ρ is the bulk density for each material. The cellulosic fiber for blue jeans and recycled cotton has a density around 1500 kg/m^3 [39]. The porosity is 0.9747 for blue jeans and 0.9653 for recycled cotton.

The contribution of solid fiber conduction is calculated as [34]

$$\lambda_F = f \bullet (1 - \phi_P) \bullet \lambda_S.\# \quad (7)$$

assuming the thickness of the material is larger than the mean free path of radiation photons, the material is optically thick, and the boundary surfaces are black. The radiation effect on the effective thermal conductivity can be expressed as [34]

$$\lambda_R = 4 \bullet \sigma_S \bullet L_0 \bullet \beta \bullet T_m{}^3. \quad (8)$$

where σ_S is the Stefan–Boltzmann constant, 5.67×10^{-8} W/(m^2·K^4); β is the opacity factor that represents the radiational properties of the fibers and fiber layers; and T_m is the mean temperature of the material determined by the measured mean temperature of the HFM, which was 297 K.

The inputs of the model included the maximum density measured by the compression test, the mean fiber diameter characterized by the SEM instrument, measured thermal conductivity as a function of air pressure, and the measured mean temperature of the upper and lower plates of the HFM during thermal conductivity measurements.

3. Results and discussion

3.1. Thermal conductivity

3.1.1. Effect of pressure

Measured thermal conductivity as a function of internal air pressure is presented in Fig. 5. Thermal conductivity dropped dramatically when the pressure decreased from ambient to approximately 5 Pa. Below 5 Pa, the reduction of thermal conductivity slowed and exhibited a tendency to reach a plateau. This observation suggests that at air pressures lower than 5 Pa, the effect of pressure on the thermal conductivities of the fiber mats diminishes; this is attributed to the limited influence of gas conduction at pressures less than 5 Pa [34,37,38,40]. Our model also shows this finding in Section 3.4 (Fig. 12). Thus, a core pressure of 5 Pa is sufficient to achieve the minimum thermal conductivity.

We found that many of these natural fiber materials are excellent candidates for VIP cores with low thermal conductivities. These natural fiber–based VIPs may need to have enough compressive strength to ensure a minimum increase in their densities when packaged in VIP with the external compressive force from ambient pressure. Their compressive strengths depend not only on the materials' mechanical properties but also on how the VIPs are manufactured, such as the mixture of natural fibers [21,30], the design of internal support structures [28], and the use of binders [41]. Typical center-panel commercially available VIPs have thermal conductivities of around 4 mW/(m·K) [42–44]. Considering the effects of thermal bridging (heat conduction across the panel edges), the overall thermal conductivity of traditional VIPs is approximately 4–8 mW/(m·K) [42–44]. Compared with the thermal performance of traditional VIPs, the natural fiber materials were divided into three categories based on their thermal conductivities in a vacuum ($p < 5$ Pa): ideal VIP candidates (<4 mW/[m·K]), excellent VIP candidates (4–8 mW/[m·K]), and less favorable candidates (>8 mW/[m·K]), as shown in Fig. 6. Recycled cotton, bamboo fiber, and kapok achieved the lowest thermal conductivities: 3.6, 1.93, and 2.79 mW/(m·K), respectively. With even lower thermal conductivities than those of conventional VIP core materials, these natural fibers are ideal candidates for VIP cores. The thermal conductivities of blue jeans, jute mat, and sheep wool batts #1, #2, and #3 were 4–8 mW/(m·K), similar to those of conventional VIPs, making these natural fibers excellent

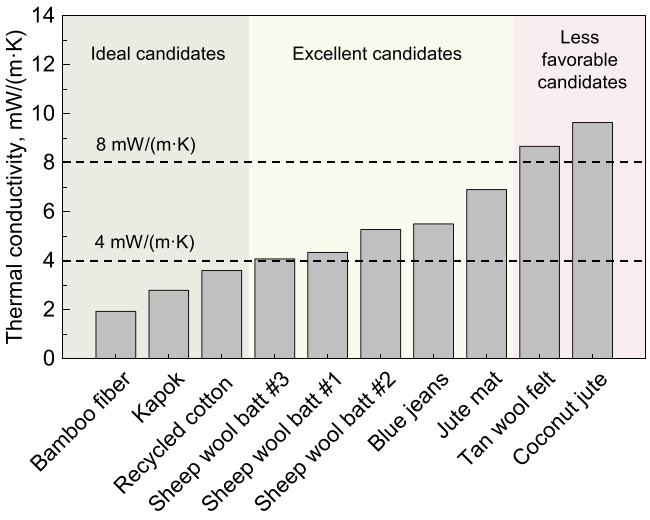

Fig. 6. Thermal conductivities of natural fibers in vacuum pressure (<5 Pa). The candidates are divided into three categories: ideal VIP candidates (<4 mW/[m·K]), excellent VIP candidates (4–8 mW/[m·K]), and less favorable candidates (>8 mW/[m·K]).

candidates for VIPs. The other two fiber mats, coconut jute and tan wool fiber, had thermal conductivities greater than 8 mW/(m·K) and thus are less favorable for use as VIP cores. Because coconut jute had the maximum thermal conductivity, which was impossible to be a potential VIP core. This material did not conduct mechanical behavior tests. Based on the initial densities in Table 1, results indicate that the ideal natural fiber candidates have low initial densities (<52 kg/m^3), whereas the less favorable natural fiber candidates have relatively high initial densities (>118 kg/m^3). Further details of thermal conductivity for each candidate group can be found in Appendix A.

A few comparisons were made between our results and the literature data shown in Fig. 7. At ambient pressure, our thermal conductivity values were 33–48 mW/(m·K), consistent with the literature data, which were 33–88 mW/(m·K) [14,19–27,45]. At vacuum levels (<5 Pa), very few literature data were found. For recycled cotton, Zach et al. obtained 3.17–5.15 mW/(m·K) at 0.1–5 Pa [26,27], which is close to our measured data (3.6–5.0 mW/[m·K]). For kapok, Sun et al. measured 6.12 mW/(m·K) with a density of 98.9 kg/m^3 at 0.5 Pa [19]. In comparison, the kapok sample in Fig. 5 had a lower thermal conductivity of 2.8 mW/(m·K) and a lower density of 46.2 kg/m^3. For bamboo fiber,

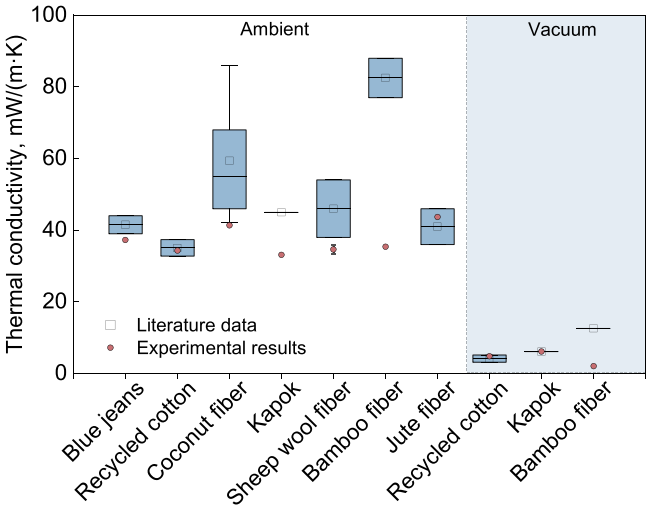

Fig. 7. Thermal conductivities of natural fibers at ambient and vacuum pressures, as found in the literature [14,19–27,45].

Dong et al. measured 12.6 mW/(m·K) at 0.05 Pa [14], which is also higher than our value of 2.0 mW/(m·K) at the same vacuum level. This may have been caused by the density difference or the fiber diameter; the bamboo fiber's density and diameter were not reported in Dong et al.'s paper. Even though comparing the thermal conductivities among different studies is difficult because of differences in fiber diameter, density, and alignments, studies have consistently found that recycled cotton and kapok have low thermal conductivities in a vacuum.

3.1.2. Effect of density at the maximum vacuum level

The effect of density on the measured thermal conductivity at the maximum vacuum level is presented in Fig. 8. Fiber mat compression (or higher density) can significantly reduce thermal conductivity. The thermal conductivity of recycled cotton as a function of density at 0.026 Pa is shown in Fig. 8(b), which displays a clear trend of thermal conductivity decreasing with increasing density. Specifically, when density increased by 40 %, thermal conductivity decreased by 18 %, from 4.3 to 3.5 mW/(m·K). This was likely caused by the reduction in radiative heat transfer owing to shrinkage of the pores as density increased. If the density continued increasing, we expect that the thermal conductivity would eventually increase because the radiative heat transfer would eventually be diminished, and the increase in solid conduction would dominate. The decrease of the thermal conductivity of fiber material with increasing density was also reported in Bankvall's work [34]. Other studies have similarly found that changes in density significantly affected the thermal conductivity of fiber material [34,40, 46–48].

3.2. Mechanical behavior under compression

Compression tests were conducted for fiber mats to quantify compressive strengths and associated density changes. These measurements were used to determine whether internal supportive structures were needed for natural fiber–based VIPs to improve thermal performance. Fig. 9 shows the stress–strain curves, each consisting of an initial linear, a subsequent nonlinear, and a final linear segment. At the initial linear segments, the strain increased rapidly under even a small compressive stress because of the fiber mats' porous structures. This represented the elastic region for fiber mats. Then, a nonlinear stress–-strain relationship was caused by the change of the original porous structure under external force. During this stage, the increment of deformation in the mat's thickness was large at the beginning and then gradually decreased. Finally, another linear stress–strain relationship was caused by the fiber mats approaching a "solid" structure with further compression. Based on the initial linear segments, the modulus

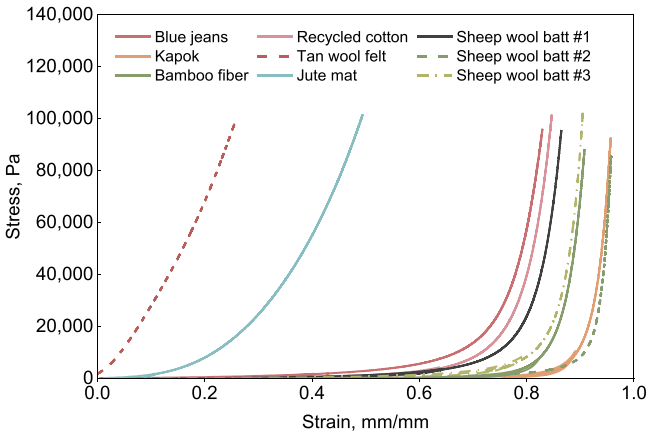

Fig. 9. Stress–strain curves of natural fiber mats under compression.

of elasticity were calculated to be in the range of 111 Pa to 0.28 MPa, as shown in Fig. 9. At ambient pressure, the strains for tan wool felt and jute mat were lower than 0.5 mm/mm, significantly lower than the strains for other natural fibers. These two materials have a much higher elastic modulus than that of the other fiber materials, indicating that tan wool felt and jute mat as VIP cores could prevent collapse under atmospheric pressure.

The densities of fiber mats under different externally applied pressures are listed in Table 1. When the externally applied pressure was 6205 Pa, the corresponding densities were 3 %–523 % higher than the initial densities without any external pressure. When the pressure reached 1 atm (101325 Pa), the densities further increased by 92 %–2702 %, except for tan wool felt, whose density increased by 27 %. Sheep wool batt #2 exhibited the most significant change in density, whereas the tan wool felt had the least noticeable change. Preserving the porous structures of fiber mats is desirable to maintain low thermal conductivity in VIP core material. Thus, except for tan wool felt, most natural fiber–based VIPs need an internal supportive structure.

3.3. Morphology of natural fibers

The morphology of natural fiber plays a significant role in the performance of a VIP fiber mat, hence affecting thermal conductivity. Fig. 10 shows the surface microstructures of the fiber mats. Among the ideal candidates, kapok and recycled cotton appear as warped straws, and bamboo fiber looks like a bundle of many tubes. Among the excellent candidates, the sheep wool batts (animal fibers) have clear fish

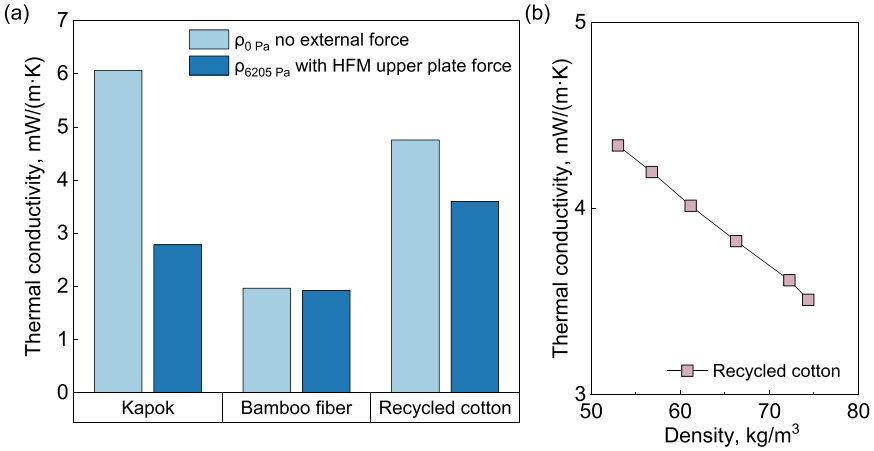

Fig. 8. Measured density-dependent thermal conductivity at the maximum vacuum level: (a) the measured thermal conductivities with two densities (ρ_{0Pa} and ρ_{6205Pa}) for kapok, bamboo fiber, and recycled cotton; (b) the measured thermal conductivities for recycled cotton with four additional density intervals generated by the 6205 Pa external compressive force that decreased the manual thickness from 35.56 to 27.16 mm.

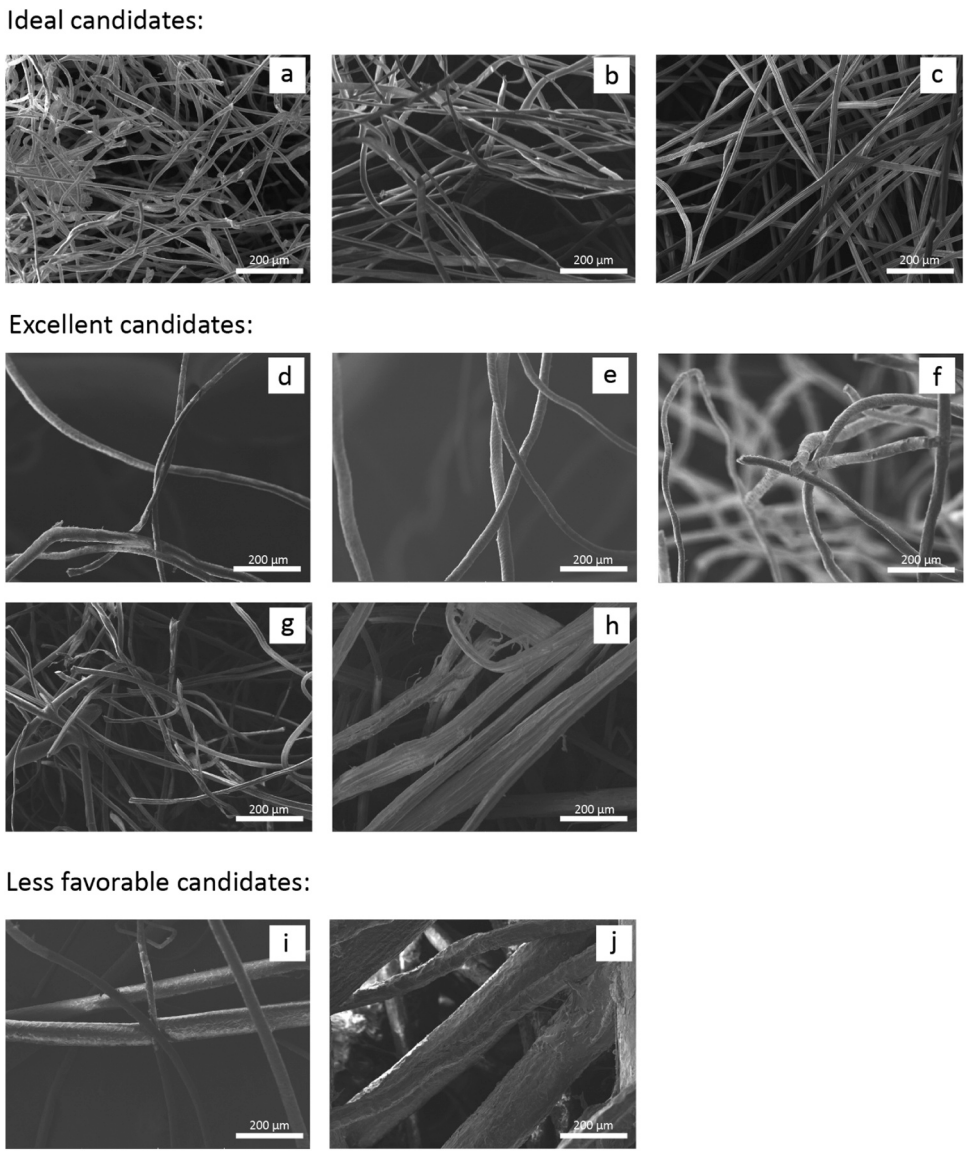

Fig. 10. SEM images of natural fibers: (a) recycled cotton, (b) kapok, (c) bamboo fiber, (d) sheep wool batt #1, (e) sheep wool batt #2, (f) sheep wool batt #3, (g) blue jeans, (h) jute mat, (i) tan wool felt, and (j) coconut jute.

scale–like structures, whereas a circular structure can be seen in blue jeans, and the fibril structure of jute mat has crumples. Of the less favorable candidates, tan wool felt has a fish-scale appearance similar to that of the sheep wool batts but with a larger diameter; coconut jute has the largest diameter of the fibers and has a circular structure. The irregular surfaces of natural fibers may prevent contact with adjacent fibers and create more porous space, which could affect the thermal conductivity of the VIP [19].

The diameters of natural fibers affect the thermal conductivity of VIPs, thus affecting gas conduction and radiation in the fiber mat [34]. When the fiber diameter is small, the mean fiber distance is reduced, as indicated by Eq. (4). As a result, gas conduction and radiative heat transfer decrease, leading to a corresponding decrease in effective thermal conductivity of the natural fiber–based VIP. The average diameters of the tested natural fibers ranged from 12.8 to 182.9 μm (Table 2). The average diameters for most of the fibers were less than 59.3 μm. A reduction in fiber diameter resulted in a decrease in the average fiber distance, hence decreasing gas conduction and radiation and leading to lower total thermal conductivity [34].

As shown in Fig. 11, for the natural fiber–based VIP design, the ideal natural fibers had small fiber diameters (less than approximately 18 μm), whereas the less favorable fibers had large mean fiber diameters (>183 μm) and much higher fiber mat densities compared with those of the other fibers. As seen in Table 1, coconut jute and tan wool felt had

Table 2
Modulus of elasticity and fiber diameters.

Material	Modulus of elasticity (Pa)	Diameter (μm)	
		Average	Standard deviation
Blue jeans	4384	16.6	5.8
Recycled cotton	1653	12.8	4.4
Tan wool felt	280,080	39.1	20.0
Coconut jute	N/A[a]	182.9	103.0
Kapok	111	16.8	5.0
Sheep wool batt #1	1802	24.8	8.2
Sheep wool batt #2	509	36.5	9.3
Sheep wool batt #3	1099	31.0	7.9
Bamboo fiber	271	18.1	3.4
Jute mat	15,663	59.3	25.0

[a]Compression testing was not performed on coconut jute because of its poor thermal performance compared with that of other materials. (described in Section 3.1.1).

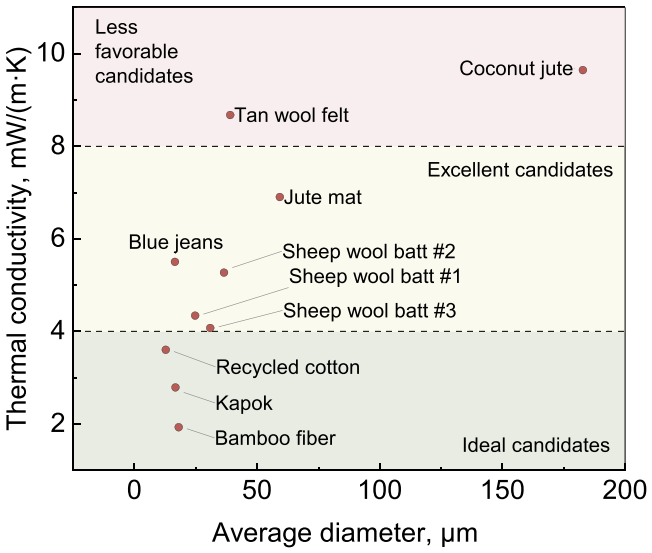

Fig. 11. Thermal conductivity as a function of fiber diameter.

densities of 118 and 190 kg/m^3, respectively, which were much higher than the densities of the other measured fiber mats.

3.4. Modeling results

The model estimates four unknown parameters: thermal conductivity of the solid phase, λ_S; porosity structure parameters in series, ϕ_S; porosity structure parameters in parallel, ϕ_P; and opacity factor, β. Bayesian optimization was used to determine these unknown parameters with given experimental data based on Eqs. (1)–(8). The mean squared error (MSE) was used to measure the model's accuracy. The estimated parameters and the experimental data are listed in Table 3.

Fig. 12 compares the modeling results with our experimental results for blue jeans and recycled cotton. The MSEs for blue jeans and recycled cotton were 1.26 × 10^{-5} W^2/(m^2·K^2) and 1.73 × 10^{-4} W^2/(m^2·K^2), respectively, demonstrating good model performance. The challenge of this model was to predict the thermal conductivity at ambient pressure, which was predominantly influenced by the gas conductivity. Therefore, the simulated gas conductivity was lower than that of the measurements at ambient pressure. Further studies will be necessary to improve accuracy.

Some deviations between the predictions and the experimental data were observed. These may be attributed partly to ignoring the coupling effects in the modeling. The coupling effect is a second-order phenomenon influenced by fiber properties, pressure, and temperature [38,49]. The high thermal conductivity at vacuum pressure may be attributed partly to short-circuiting cuts induced by air conduction in coupling effect [37]. Because of its complexity, the coupling effect is not considered in this study.

Table 3
Model parameters and accuracies (MSEs).

Parameter	Fiber material	
	Blue jeans	Recycled cotton
D (μm)	16.6	12.8
ρ_s (kg/m^3)	1500	1500
ϕ	0.9747	0.9653
ϕ_S	0.9441	0.8211
ϕ_P	0.9968	0.9654
λ_S (W/[m·K])	0.0999	0.0606
β	1.2042	0.3168
f	0.5802	0.9991
MSE (W^2/[m^2·K^2])	1.26 × 10^{-5}	1.73 × 10^{-4}

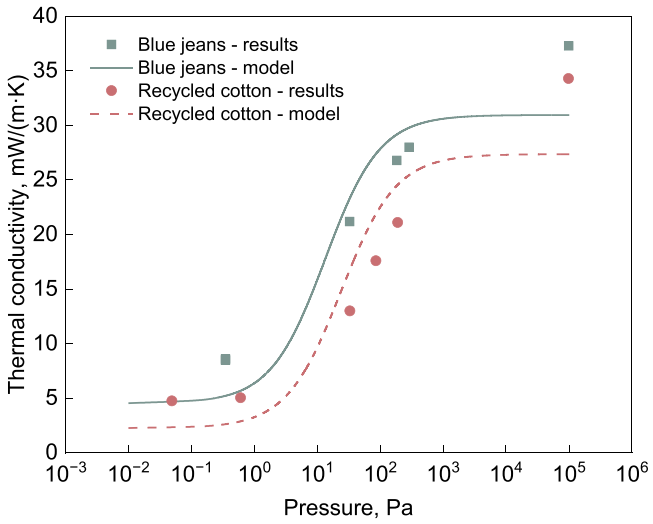

Fig. 12. Simulated thermal conductivity as a function of internal gas pressure for blue jeans and recycled cotton, with fixed density.

3.4.1. Effect of internal air pressure on heat transfer mechanisms

The calibrated model was used to study the effects of vacuum pressure on mechanisms of heat transfer in blue jeans and recycled cotton. Fig. 13 presents the contributions of gas conduction, solid conduction of fiber, and radiation to effective thermal conductivity from ambient pressure to the maximum vacuum pressure.

At ambient pressure, the effective thermal conductivity was dominated by gas conduction for both blue jeans and recycled cotton, as expected. The second-highest contributors were radiation for blue jeans and fiber conduction for recycled cotton. This difference was because blue jeans had a higher opaque factor, whereas recycled cotton had a close-to-series structure (higher f), which increased fiber conduction. At pressures greater than approximately 2 Pa, the fractions contributed by gas conduction varied from 0.48 to 0.85 for blue jeans and from 0.52 to 0.91 for recycled cotton.

At vacuum levels, as the contribution from gas conduction decreased, the dominant contributors were radiation for blue jeans and fiber conduction for recycled cotton. When the pressure was reduced to 10^{-2} Pa, the fraction contributed by radiation was 0.96 for blue jeans, and the fraction contributed by fiber conduction was 0.91 for recycled cotton.

The results suggest that as pressure changes from ambient to vacuum levels, the dominant heat transfer mechanism shifts from gas conduction to radiation and fiber conduction. Moreover, when the pressure was

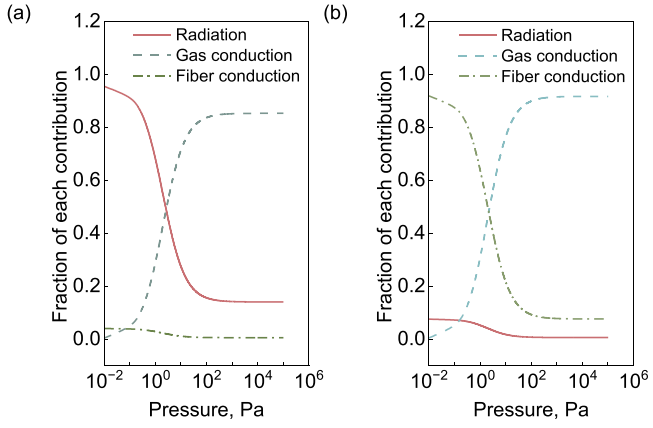

Fig. 13. Fraction contributed to effective thermal conductivity as a function of internal air pressure for gas conduction, fiber conduction, and radiation: (a) blue jeans and (b) recycled cotton.

reduced to around 5 Pa, the effective thermal conductivity decreased slowly.

4. Summary

This study measured thermal conductivities, compression properties, and fiber diameters of 10 natural fibers to identify potential candidates for VIP core materials. Fiber selection criteria were discussed for natural fiber–based VIPs that can offer cost-effectiveness, sustainability, and energy-efficiency benefits. The findings from our research have important implications for the development of environmentally friendly, high-performance insulation materials.

Among the tested natural fibers, recycled cotton, kapok, and bamboo fiber had the lowest thermal conductivities at vacuum and hence were found to be ideal candidates for VIP core materials. They exhibited lower thermal conductivities than those of traditional VIPs with fumed silica cores at high vacuum. Additionally, blue jeans, sheep wool batts, and jute mat were deemed excellent candidates for VIP applications, offering thermal conductivities similar to those of traditional VIPs at much lower cost. Conversely, our investigation revealed that coconut shell jute, with the largest fiber diameter, and tan wool felt, with the highest density among the tested materials, were not suitable as VIP core materials because of their high thermal conductivities. Furthermore, we discovered that for recycled cotton, an increase in density of up to 40 % of the initial density resulted in an 18 % improvement in thermal conductivity at vacuum.

5. Conclusion

Designing natural fiber–based VIPs with low thermal conductivity has several key considerations: the criteria for selecting an ideal natural fiber as a VIP core, internal air pressure after packaging, and necessity of VIP internal supportive structures. First, based on our measurement, the ideal natural fiber for this application has a small fiber diameter (less than approximately 18 μm) and a low fiber mat density (below 52 kg/m^3). Second, although a core pressure of 5 Pa is sufficient to attain the minimum thermal conductivity, the recommendation for prolonged service life is to obtain an internal air pressure below 5 Pa to account for gas diffusion through VIP package barrier films and potential off-gassing from fibers. Last, assessing the necessity of supportive structures is crucial to prevent the natural fiber mat from developing a solid structure, which could compromise thermal performance.

Future work

Studying aging effects on the thermal conductivity of natural fiber–based VIPs and life cycle analysis will be essential under different exposure environments involving the effects of humidity and temperature. Natural fibers are susceptible to off-gassing and mold growth. The VIP manufacture process must use desiccators and getters to adsorb the moisture and off-gassing from the fibers or diffuse them through barrier film. Additional requirements may include designing effective supportive structures or innovating a new VIP core by using different combinations of natural fibers with or without binders to obtain a high compressive strength.

CRediT authorship contribution statement

Bokyung Park: Investigation, Data curation. **Tianli Feng:** Writing – review & editing, Formal analysis, Data curation. **Rui Zhang:** Writing – review & editing, Writing – original draft, Investigation, Formal analysis, Data curation, Conceptualization. **Zhenglai Shen:** Writing – review & editing, Methodology, Investigation. **Som Shrestha:** Writing – review & editing, Supervision, Resources, Project administration, Methodology, Investigation, Funding acquisition, Formal analysis, Conceptualization. **Diana Hun:** Writing – review & editing, Funding acquisition, Conceptualization. **Antonio Aldykiewicz Jr:** Writing – review & editing, Investigation, Conceptualization. **André Desjarlais:** Writing – review & editing, Investigation, Conceptualization.

Declaration of Competing Interest

The authors declare that they have no known competing financial interests or personal relationships that could have appeared to influence the work reported in this paper.

Acknowledgments

This research was supported by the US Department of Energy's (DOE's) Office of Energy Efficiency and Renewable Energy (EERE) Building Technologies Office under Contract No. DE-AC05–00OR22725 with UT-Battelle, LLC, and used resources at the Building Technologies and Research Integration Center, a DOE EERE User Facility at DOE's Oak Ridge National Laboratory.

Appendix A

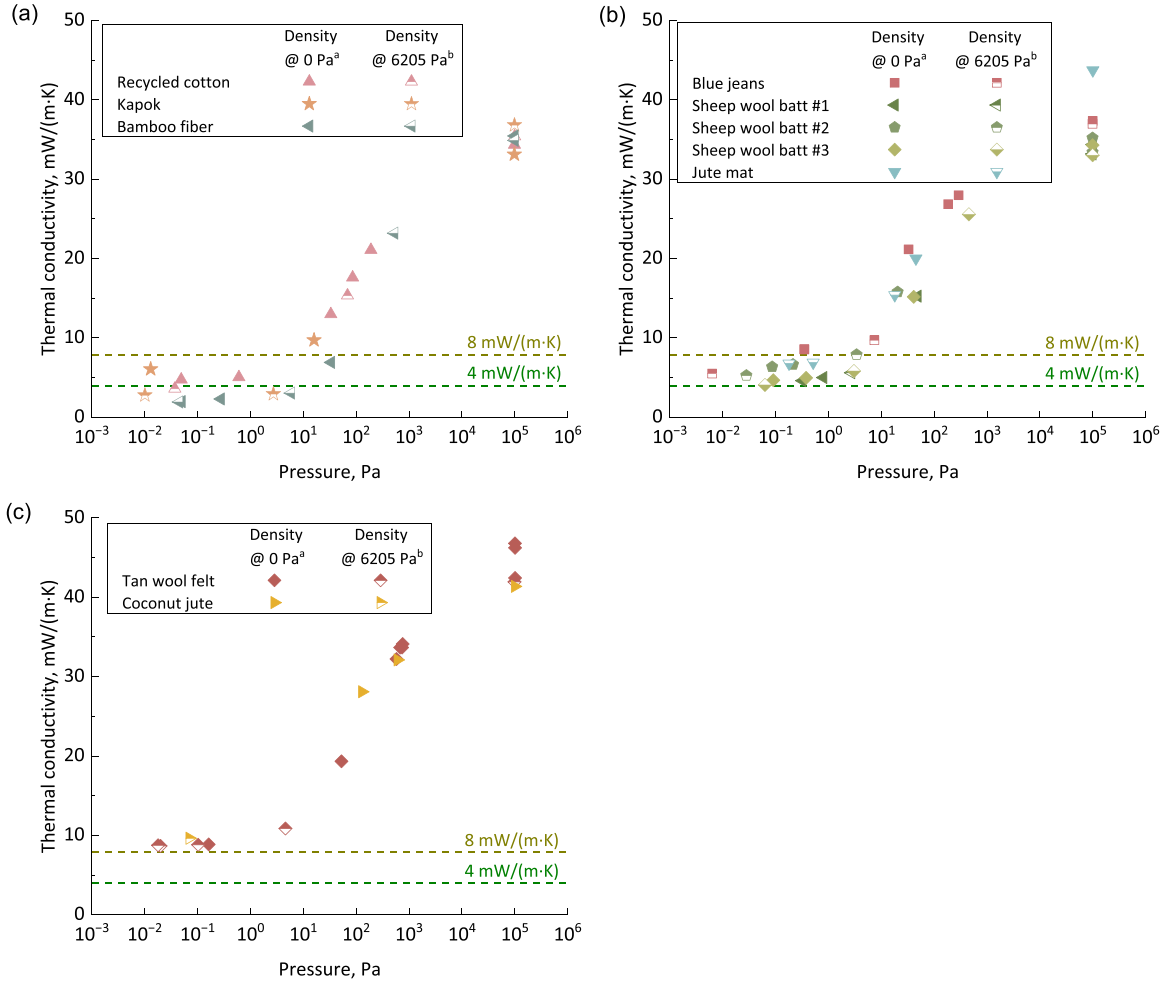

Fig. A-1. provides the details of thermal conductivity for each candidate group. A-1. Measured pressure-dependent thermal conductivities for (a) ideal candidates, (b) excellent candidates, and (c) less favorable candidates.

Data availability

Data will be made available on request.

References

[1] F. Sheet, President Biden Sets 2030 Greenhouse gas pollution reduction target aimed at creating good-paying union jobs and securing US leadership on clean energy technologies, The White House, 2021.

[2] J.R. Zhao, R. Zheng, J. Tang, H.J. Sun, J. Wang, A mini-review on building insulation materials from perspective of plastic pollution: current issues and natural fibres as a possible solution, J. Hazard. Mater. (2022) 129449.

[3] F. Mostafavi, M. Tahsildoost, Z. Zomorodian, Energy efficiency and carbon emission in high-rise buildings: a review (2005-2020), Build. Environ. 206 (2021) 108329.

[4] B. Wang, et al., Thermal insulation properties of green vacuum insulation panel using wood fiber as core material, BioResources 14 (2) (2019) 3339–3351.

[5] R. Baetens, et al., Vacuum insulation panels for building applications: a review and beyond, Energy Build. 42 (2) (2010) 147–172.

[6] M. Alam, H. Singh, S. Suresh, D. Redpath, Energy and economic analysis of Vacuum Insulation Panels (VIPs) used in non-domestic buildings, Appl. Energy 188 (2017) 1–8.

[7] A. Uriarte, I. Garai, A. Ferdinando, A. Erkoreka, O. Nicolas, E. Barreiro, Vacuum insulation panels in construction solutions for energy efficient retrofitting of buildings. Two case studies in Spain and Sweden, Energy Build. 197 (2019) 131–139.

[8] S.S. Alotaibi, S. Riffat, Vacuum insulated panels for sustainable buildings: a review of research and applications, Int. J. Energy Res. 38 (1) (2014) 1–19.

[9] S. Song, Q. Wang, M. Zhang, Bamboo fiber-based insulating paper: a potential choice towards greener power and paper industries, BioResources 18 (2) (2023) 2528.

[10] N. Ijjada, R.R. Nayaka, Review on properties of some thermal insulating materials providing more comfort in the building, Mater. Today. Proc. (2022).

[11] P. Johansson. Vacuum insulation panels in buildings: Literature review, 2012.

[12] M. Alam, H. Singh, M. Limbachiya, Vacuum Insulation Panels (VIPs) for building construction industry–a review of the contemporary developments and future directions, Appl. Energy 88 (11) (2011) 3592–3602.

[13] E. Department. Inexpensive and Durable Aerogel-Based VIP Cores. http://www.energy.gov/eere/buildings/articles/inexpensive-and-durable-aerogel-based-vip-cores-0 (accessed September 26, 2023..

[14] X. Dong, et al., Preparation and characterization of vacuum insulation panels with hybrid composite core materials of bamboo and glass fiber, Ind. Crops Prod. 188 (2022) 115691.

[15] J.-S. Kwon, C.H. Jang, H. Jung, T.-H. Song, Vacuum maintenance in vacuum insulation panels exemplified with a staggered beam VIP, /05/01/ 2010, Energy Build. 42 (5) (2010) 590–597, https://doi.org/10.1016/j.enbuild.2009.10.029.

[16] D. Tetlow, et al., Cellulosic-crystals as a fumed-silica substitute in vacuum insulated panel technology used in building construction and retrofit applications, Energy Build. 156 (2017) 187–196.

[17] R. Merget, et al., Health hazards due to the inhalation of amorphous silica, Arch. Toxicol. 75 (2002) 625–634.

[18] C.E. Njoku, K.K. Alaneme, J.A. Omotoyinbo, M.O. Daramola, Natural fibers as viable sources for the development of structural, semi-structural, and technological materials–a review, Adv. Mater. Lett. 10 (10) (2019) 682–694.

[19] Q. Sun, et al., Green and sustainable kapok fibre as novel core materials for vacuum insulations panels, Appl. Energy 347 (2023) 121394.

[20] F. Asdrubali, F. D'Alessandro, S. Schiavoni, A review of unconventional sustainable building insulation materials, Sustain. Mater. Technol. 4 (2015) 1–17, https://doi.org/10.1016/j.susmat.2015.05.002.

[21] J. Zach, J. Peterková, Z. Dufek, T. Sekavčnik, Development of vacuum insulating panels (VIP) with non-traditional core materials, Energy Build. 199 (2019) 12–19, https://doi.org/10.1016/j.enbuild.2019.06.026.
[22] S. Schiavoni, F. Bianchi, F. Asdrubali, Insulation materials for the building sector: a review and comparative analysis, Renew. Sustain. Energy Rev. 62 (2016) 988–1011.
[23] M. Zakriya, G. Ramakrishnan, N. Gobi, N. Palaniswamy, J. Srinivasan, Jute-reinforced non-woven composites as a thermal insulator and sound absorber–a review, J. Reinf. Plast. Compos. 36 (3) (2017) 206–213.
[24] S. Panyakaew, S. Fotios, New thermal insulation boards made from coconut husk and bagasse, Energy Build. 43 (7) (2011) 1732–1739, https://doi.org/10.1016/j.enbuild.2011.03.015.
[25] D. Kumar, M. Alam, P.X. Zou, J.G. Sanjayan, R.A. Memon, Comparative analysis of building insulation material properties and performance, Renew. Sustain. Energy Rev. 131 (2020) 110038.
[26] A. Kan, X. Zhang, Z. Chen, D. Cao, Effective thermal conductivity of vacuum insulation panels prepared with recyclable fibrous cotton core, Int. J. Therm. Sci. 187 (2023) 108176.
[27] J. Zach, J. Peterková, V. Novák, Urilization of natural-based row sources for vacuum insulation production, Int. Multidiscip. Sci. GeoConference: SGEM 18 (6.3) (2018) 445–452.
[28] B. Choi, I. Yeo, J. Lee, W.K. Kang, T.-H. Song, Pillar-supported vacuum insulation panel with multi-layered filler material, Int. J. Heat. Mass Transf. 102 (2016) 902–910.
[29] J.P. Vitale, G. Francucci, A. Stocchi, Thermal conductivity of sandwich panels made with synthetic and vegetable fiber vacuum-infused honeycomb cores, J. Sandw. Struct. Mater. 19 (1) (2017) 66–82.
[30] C.D. Li, Z.F. Chen, Novel honeycomb glassfiber mat as the core of vacuum insulation panel, Adv. Mater. Res. 900 (2014) 247–250.
[31] V.K. Thakur, M.K. Thakur, R.K. Gupta, Raw natural fiber–based polymer composites, Int. J. Polym. Anal. Charact. 19 (3) (2014) 256–271.
[32] Standard Test Method for Steady-State Thermal Transmission Properties by Means of the Heat Flow Meter Apparatus, A. S. C518-521, 2021.
[33] Standard Test Method for Measuring Compressive Properties of Thermal Insulations, A. S. C165-23, 2023.
[34] C.G. Bankvall, Heat transfer in fibrous materials. 1972.
[35] H. Schwab, U. Heinemann, A. Beck, H.-P. Ebert, J. Fricke, Dependence of thermal conductivity on water content in vacuum insulation panels with fumed silica kernels, J. Therm. Envel. Build. Sci. 28 (4) (2005) 319–326.
[36] J. Zhuang, S.H. Ghaffar, M. Fan, J. Corker, Restructure of expanded cork with fumed silica as novel core materials for vacuum insulation panels, Compos. Part B Eng. 127 (2017) 215–221.
[37] C.M. Pelanne, Heat flow principles in thermal insulations, J. Therm. Insul. 1 (1) (1977) 48–80.
[38] S.S. Shrestha, et al., Solid and gas thermal conductivity models improvement and validation in various porous insulation materials, Int. J. Therm. Sci. 187 (2023) 108164.
[39] S.N. Athey, et al., The widespread environmental footprint of indigo denim microfibers from blue jeans, Environ. Sci. Technol. Lett. 7 (11) (2020) 840–847.
[40] K. Manohar, G.S. Kochhar, Experimental investigation of the influence of air conduction on heat transfer across fibrous materials, J. Mech. Eng. Res 3 (2011) 24–319.
[41] Q. Sun, et al., Functionalising kapok fibre with lignin to enhance the structural and thermal performance of vacuum insulation panels, Ind. Crops Prod. 220 (2024) 119277.
[42] A. Kan, X. Zhang, Z. Chen, D. Cao, Effective thermal conductivity of vacuum insulation panels prepared with recyclable fibrous cotton core, Int. J. Therm. Sci. 187 (2023), https://doi.org/10.1016/j.ijthermalsci.2023.108176.
[43] Q. Sun, et al., Green and sustainable kapok fibre as novel core materials for vacuum insulations panels, Appl. Energy 347 (2023), https://doi.org/10.1016/j.apenergy.2023.121394.
[44] S.E. Kalnæs, B.P. Jelle, Vacuum insulation panel products: a state-of-the-art review and future research pathways, Appl. Energy 116 (2014) 355–375.
[45] O. Kaynakli, A review of the economical and optimum thermal insulation thickness for building applications, Renew. Sustain. Energy Rev. 16 (1) (2012) 415–425.
[46] C. Stark, J. Fricke, Improved heat-transfer models for fibrous insulations, Int. J. Heat. Mass Transf. 36 (3) (1993) 617–625.
[47] R.K. Bhattacharyya, Heat-transfer model for fibrous insulations, ASTM International, 1980.
[48] P. Rebolledo, A. Cloutier, M.-C. Yemele, Effect of density and fiber size on porosity and thermal conductivity of fiberboard mats, Fibers 6 (4) (2018) 81.
[49] F. Favoino, Simulation-based evaluation of adaptive materials for improved building performance. In: Nano and Biotech Based Materials for Energy Building Efficiency, pp. 125-166, 2016.